

Statistical Analysis of Electrical Properties of Octanemonothiol versus Octanedithol in PEDOT:PSS-Electrode Molecular Junctions

Hanki Lee, Hyunhak Jeong, Dongu Kim, Wang-Taek Hwang, Youngbin Tchoe, Gyu-Chul Yi, and Takhee Lee*

Department of Physics and Astronomy, Seoul National University, Seoul 151-747, Korea

We fabricated a large number of octanemonothiol (C8) and octanedithol (DC8) molecular electronic devices with PEDOT:PSS (3,4-ethylenedioxythiophene) interlayer and performed a statistical analysis on the electronic properties of these devices. From the analysis, we obtained the Gaussian plot of histograms of Log_{10} (current density (J)) and several statistical estimates such as arithmetic mean, median, Gaussian mean, arithmetic standard deviation, adjusted absolute median deviation, and Gaussian standard deviation. We determined the current density–voltage (J – V) characteristics from the statistically representative data for C8 and DC8 devices and found that the conductivity of C8 is higher than that of DC8 by a factor of ~ 10 . The difference of the conductivity of C8 and DC8 devices is attributed to the difference of the contact properties between the C8 and DC8 PEDOT:PSS-interlayer molecular junctions.

Keywords: Molecular Devices, PEDOT:PSS, Statistical Analysis.

1. INTRODUCTION

The fabrication of molecular electronic junction using a conductive polymer (PEDOT:PSS; 3,4-ethylenedioxythiophene) between the top electrode and the molecules has been one of the most successful techniques in terms of high device yields and stable junctions.¹ Nevertheless, the use of a conductive polymer presents some uncertainties as a platform for molecular devices because the properties of the interface between the polymer layer and the molecules are not thoroughly understood.^{1–6} Therefore, more detailed understanding of the interface between the polymer layer and the molecules should be done in the field of molecular electronics.

In this study, we fabricated sufficient number of octanemonothiol (C8; 112 devices) and octanedithol (DC8; 128 devices) molecular devices with PEDOT:PSS interlayer for a meaningful statistical analysis. First, we measured the electrical properties of the fabricated molecular devices and made histograms of Log_{10} |current density (J)|. Next, we performed a statistical analysis

and obtained several statistical estimates; arithmetic mean (μ_A), median (μ_M), Gaussian mean (μ_G), arithmetic standard deviation (σ_A), adjusted absolute median deviation (σ_M), and Gaussian standard deviation (σ_G). Then, we compared the conductivity of C8 devices with DC8 devices from the current density–voltage (J – V) characteristics. Finally, we discussed the relation between the conductivity and the contact properties in C8 and DC8 devices to understand the difference in the electrical characteristics.

2. EXPERIMENTAL DETAILS

The Au-octanethiol-PEDOT:PSS/Au junctions were fabricated on a p -type (100) 300 nm thickness SiO_2 substrate. First, patterned Au(500 Å)/Ti (100 Å) bottom electrodes were formed on the SiO_2 substrate using a shadow mask by an electron beam evaporator at a deposition rate of ~ 0.1 Å/s. Next, photoresist (AZ5214) was spin coated on the bottom electrodes to form an insulating wall which electrically isolates the bottom electrodes with the top electrodes. And then, via-hole structures in the photoresist layer were generated. The via-holes were square-shaped and the side lengths of the holes ranged from 30 μm to

* Author to whom correspondence should be addressed.

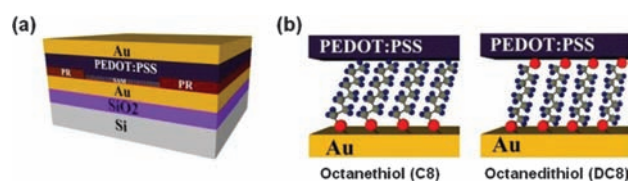


Figure 1. (a) A schematic diagram of the device structure of our molecular devices. (b) Molecular structures of C8 and DC8. In C8 devices, methyl ($-\text{CH}_3$) end group contacts with PEDOT:PSS layer whereas in DC8 devices, thiol ($-\text{S}$) end group contacts with PEDOT:PSS layer.

100 μm with an increment of 10 μm . After the formation of the via-holes, the devices were annealed on a hot plate at $\sim 200^\circ\text{C}$ for 2 h 30 min to make the photoresist layer insoluble in ethanol during the formation of the molecular self-assembled monolayer (SAM) on the bottom electrodes. Subsequently, the devices were put into 2 mM octanemonothiol (C8) and octanedithiol (DC8) solutions diluted with ethanol for 24 h to deposit the SAMs on the bottom electrodes. After that, the devices were rinsed with ethanol to remove residual unbounded molecules. PEDOT:PSS (PH 1000 from CLEVIOSTM) was spin coated on the devices and then Au top electrodes (500 \AA) were deposited on top of the PEDOT:PSS interlayer using a shadow mask in an electron beam evaporator with the same deposition rate as the case of depositing bottom electrodes. Finally, to prevent the formation of a direct current path through the PEDOT:PSS layer between the top and bottom Au electrodes, reactive ion etching (RIE) was performed with O_2 gas to remove redundant PEDOT:PSS layers on the devices.⁷ Figure 1 shows the schematic diagram of the device structure of the molecular devices and molecular structures of C8 and DC8. The J - V characteristics of the fabricated molecular devices were measured by using a semiconductor parameter analyzer (Keithley 4200-SCS) in N_2 gas filled glove box to prevent the degradation by water vapor and O_2 .

3. RESULTS AND DISCUSSION

3.1. Statistical Analysis of Logarithmic Current Density ($\text{Log}_{10}J$) of C8 and DC8 Molecular Devices

The statistical approach to molecular electronic devices can provide a useful way to distinguish the transport property of different molecular system.⁸ Therefore we fabricated sufficient number of devices (112 C8 devices and 128 DC8 devices) for the statistical analysis and performed the analysis based on the data from the fabricated devices.

Figure 2(a) shows a histogram of $\text{Log}_{10}J$ values measured at 1 V from all data of C8 molecular devices. The 'working' devices were extracted from the devices showing a majority of current densities in the statistical distribution by using a Gaussian function.⁹ Here we selected the 99.7% of the devices from overall population which were included in the interval of the $3\sigma_G$ range

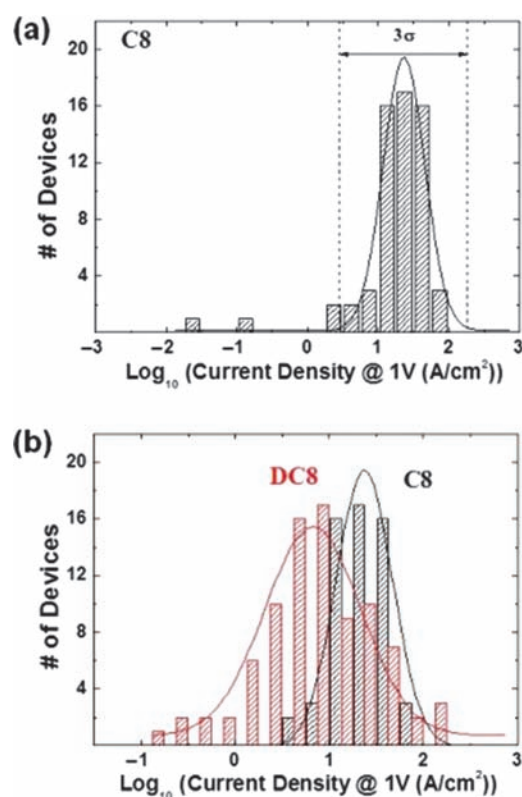


Figure 2. (a) Histogram of logarithmic current densities at 1 V from C8 molecular devices. (b) Histogram of logarithmic current densities at 1 V for C8 and DC8 devices.

between $\mu_G + 3\sigma_G$ and $\mu_G - 3\sigma_G$ as our previous report.⁸ Figure 2(b) shows the histograms of $\text{Log}_{10}J$ of working C8 and DC8 molecular devices chosen by the above restriction. With this criteria for the working devices, we determined that 61 working C8 devices and 89 working DC8 working devices, therefore the device yield was $61/112 = 54.5\%$ for C8 devices and $89/128 = 69.5\%$ for DC8 devices in PEDOT:PSS-electrode molecular junction structure. This yield is significantly larger as compared with the case of metal-molecule-metal junction structure without using PEDOT:PSS interlayer which showed a typical device yield of $\sim 1\%$.⁸

It is well known that the current density (J) through alkanethiol SAMs follows the tunneling conduction mechanism and can be expressed as;

$$J \propto \exp(-\beta d) \quad (1)$$

where d is the molecular length and β is the tunneling decay constant.¹⁰⁻²⁰ We fit the histogram data of $\text{Log}_{10}J$ with the Gaussian function as;

$$f(x) = \frac{1}{\sigma_G \sqrt{2\pi}} \exp\left[-\frac{(x - \mu_G)^2}{2\sigma_G^2}\right] \quad (2)$$

where μ_G is the Gaussian mean and σ_G is the Gaussian standard deviation. From the fittings, we could deduce statistical estimates.

For more sample statistical analysis, we calculated two more statistical estimates for the average and standard deviation: (1) arithmetic mean and (2) median by following methods:

(1) Arithmetic mean and standard deviation: Arithmetic mean (μ_A) is the sum of a collection of numbers divided by the number of numbers in the collection.²¹ Arithmetic standard deviation (σ_A) is the square root of second moment about μ_A .²²

(2) Median and median absolute deviation: The median (μ_M) is defined^{23–25} as the value for which 50% of the sample is greater than or equal to that value, and 50% of the sample is less than or equal to that value. Though median absolute deviation is useful for visualizing sample, it can't be compared directly to σ_G nor σ_A . However, for comparison with them, we can use the following adjusted median absolute deviation (σ_M).²⁶

$$\sigma_M = 1.4826 \times \text{median}(|x - \mu_M|) \quad (3)$$

The quantity, median ($|x - \mu_M|$), is called the median absolute deviation, and the factor of 1.4826 adjusts this quantity to correct for underestimation of the sample standard deviation.

Table I shows the list of these statistical estimates. As summarized in Table I, μ_G of C8 and DC8 molecular devices was found to be larger than μ_A of C8 and DC8 devices by 0.14 and 0.07, respectively. However, μ_G of C8 and DC8 devices was larger than μ_M only by 0.04 and 0.03, respectively. And, σ_G of C8 and DC8 devices were found to be smaller than σ_A of C8 and DC8 devices by 0.27 and 0.1, respectively. But σ_G of C8 and DC8 devices were smaller than σ_M of C8 and DC8 devices only by 0.02 and 0.01, respectively. These results are because μ_A and σ_A respond strongly to long tails (larger share of the data to the right of the peak than in a normal distribution) and outliers (data that lie far from the peak in histograms of $\text{Log}_{10}J$). Since most histograms had long tails and outliers, σ_A was usually found to be greater than σ_G .²²

For a true normal distribution, any estimates of the standard deviation will tend to be smaller than interquartile range (IQR) which is equal to the difference between the upper and lower quartiles.^{27,28} For the more specific analysis, we also calculated the IQR values. In our cases, IQR of C8 and DC8 molecular devices were found to be 0.42 and 0.66, respectively. Comparing them with standard deviation results in Table I, σ_M and σ_G of C8 and DC8 devices

were smaller than above IQR values. But σ_A values of C8 and DC8 devices were not smaller than IQR values. This phenomenon can be explained by that arithmetic values responded strongly to long tails and outliers in histograms of $\text{Log}_{10}J$ which were regarded as errors in the normal distribution fitting.²²

From Table I, $\text{Log}_{10}J$ of C8 was larger than that of DC8 by about 0.5 and standard deviation of C8 was smaller than that of DC8 by 0.1–0.27. The former suggests that current density of C8 is larger than that of DC8. The latter implies that the molecular contact length (d) of C8 would be shorter than that of DC8 because the distributions of $\text{Log}_{10}J$ coincide with distribution of molecular contact length from Simmons model and the standard deviation of d is normally proportional to the size of it. In other words, the larger standard deviation means the longer molecular length, therefore the larger standard deviation of DC8 devices implies the longer length of DC8 molecular junction.

3.2. Current Density–Voltage (J – V) Characteristics

Current density reflects the conductivity of different molecular systems.⁸ Here we collected the statistically representative data near from the median of J (see Fig. 2 and Table I) and plotted them in Figure 3. According to this plot, the J of C8 representative junction is higher than that of DC8 representative junction by a factor of ~ 10 in the A/cm^2 unit.

This difference of conductivity of C8 and DC8 devices is associated to their different contact properties in PEDOT:PSS-electrode molecular junction structure. Because the PEDOT:PSS does not form a chemisorbed contact with thiol-end group, the difference between C8 and DC8 junctions can be explained by a difference in the properties of the contacts corresponding to different contact lengths. Additionally, the DC8 SAM has the same ordering structure (tilt angle and packing density) as the C8 SAM on Au(111).²⁹ Thus, one possible origin of the difference in the conductivity is the shorter

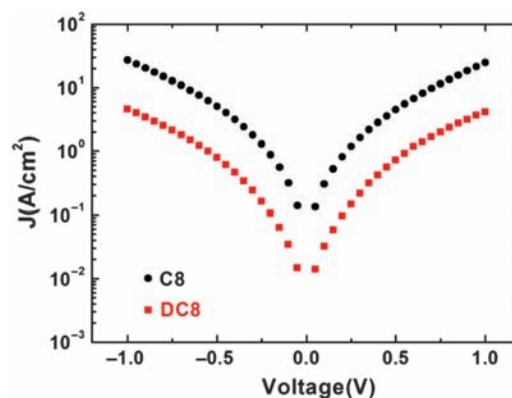


Figure 3. Current density–voltage (J – V) characteristics of octanemonthiol (C8) and octanedithiol (DC8).

Table I. The list of statistical estimates for C8 and DC8 devices.

	μ_A	μ_M	μ_G	σ_A	σ_M	σ_G
C8	1.24	1.34	1.38	0.56	0.31	0.29
DC8	0.77	0.81	0.84	0.66	0.57	0.56

Notes: μ_A : Arithmetic mean; μ_M : Median; μ_G : Gaussian mean; σ_A : Arithmetic standard deviation; σ_M : Adjusted absolute median deviation; σ_G : Gaussian standard deviation. The unit of μ_A , μ_M , and μ_G is $\text{Log}_{10}(\text{A}/\text{cm}^2)$.

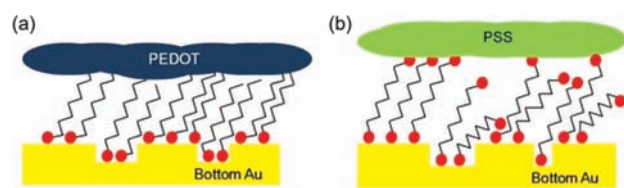


Figure 4. Schematic representation of (a) hydrophobic contact: C8-PEDOT and (b) hydrophilic contact: DC8-PSS.

length in the C8 junctions.² To explain this conclusion more precisely, we have to discuss contact properties between PEDOT:PSS interlayer and C8 or DC8. From a scanning tunneling microscopy (STM) study of a spin-coated PEDOT:PSS film, it is known that high conducting PEDOT-rich pancakes with a thickness of a few nanometers and a diameter of a few tens of nanometers are separated by non-conducting PSS lamellas.³⁰ Therefore, we can assume that the conductivity of the junction will be higher when molecules make contact with PEDOT-rich area rather than PSS. Figure 4 is the schematic representations of C8 with hydrophobic methyl contact to high conducting PEDOT part and DC8 with hydrophilic thiol contact to non-conducting PSS part. C8 and DC8 make contacts with the bottom electrodes with thiol end group ($-S$), but the other end of C8 and DC8 which are coated with PEDOT:PSS makes different contacts due to the end group of each type of molecules: i.e., C8 has hydrophobic methyl ($-CH_3$) as the end group whereas DC8 has hydrophilic thiol ($-S$) as the end group. And because PEDOT is hydrophobic and PSS is hydrophilic as we mentioned above, we can infer that the hydrophobic methyl of C8 would prefer to make contact with hydrophobic PEDOT part than hydrophilic PSS part. On the other hand, compared with the C8 case, the hydrophilic thiol of DC8 would adjoin with more hydrophilic PSS part than hydrophobic PEDOT part. This different contact (methyl-PEDOT and thiol-PSS) property can be as on why the conductivity of C8 devices is higher than that of DC8 devices. If thiol adjoins with PSS part, PSS would be less conducting than PEDOT in this case. Therefore, the conductivity of the DC8-PSS junction is relatively lower than C8-PEDOT junction.

4. CONCLUSION

We performed a statistical analysis on the electrical properties of C8 and DC8 devices fabricated in the PEDOT:PSS-electrode molecular electronic junction structure. From the statistical analysis, we could obtain several statistical estimates of C8 and DC8 devices. In particular, we observed the average of $\text{Log}_{10}J$ of C8 was larger than that of DC8 and the standard deviation of C8 was smaller than that of DC8. The latter implies that the molecular contact length of DC8 is longer than C8. From statistically representative J - V characteristics, we found that the current density of C8 is higher than that of DC8 by a factor ~ 10 .

This result is originated from different contact properties between molecules (C8 and DC8) and PEDOT:PSS interlayer. We suggest the origin of the difference in the conductivity is that C8 devices with hydrophobic methyl ($-CH_3$) as an end group make contact more easily with hydrophobic PEDOT (more conductive) part while DC8 with hydrophilic thiol ($-S$) make contact more easily with hydrophilic PSS (less conductive) part.

Acknowledgment: The authors appreciate financial support from the National Creative Research Laboratory program (Grant No. 2012026372) and the National Core Research Center program (Grant No. R15-2008-006-03002-0) through the National Research Foundation of Korea (NRF) funded by the Korean Ministry of Science, ICT and Future Planning.

References and Notes

- H. B. Akkerman, P. W. M. Blom, D. M. de Leeuw, and B. de Boer, *Nature* 441, 69 (2006).
- G. Wang, Y. Kim, M. Choe, T. W. Kim, and T. Lee, *Adv. Mater.* 23, 755 (2011).
- P. A. Van Hal, E. C. P. Smits, T. C. T. Geuns, H. B. Akkerman, B. C. De Brito, S. Perissinotto, G. Lanzani, A. J. Kronemeijer, V. Geskin, J. Cornil, P. W. M. Blom, B. De Boer, and D. M. De Leeuw, *Nat. Nanotechnol.* 3, 749 (2008).
- C. A. Nijhuis, W. F. Reus, and G. M. Whitesides, *J. Am. Chem. Soc.* 131, 17814 (2009).
- H. B. Akkerman and B. de Boer, *J. Phys.: Condens. Matter* 20, 013001 (2008).
- G. Wang, H. Yoo, S. I. Na, T. W. Kim, B. Cho, D.-Y. Kim, and T. Lee, *Thin Solid Films* 518, 4 (2009).
- S. Park, G. Wang, B. Cho, Y. Kim, S. Song, Y. Ji, M. H. Yoon, and T. Lee, *Nat. Nanotechnology* 7, 438 (2012).
- T. W. Kim, G. N. Wang, H. Lee, and T. Lee, *Nanotechnology* 18, 315204 (2007).
- H. Yoo, J. Choi, G. Wang, T. W. Kim, J. Noh, and T. Lee, *J. Nanosci. Nanotechnol.* 9, 12 (2009).
- L. A. Bumm, J. J. Arnold, T. D. Dunbar, D. L. Allara, and P. S. J. Weiss, *J. Phys. Chem. B* 103, 8122 (1999).
- B. Xu and N. J. Tao, *Science* 301, 1221 (2003).
- D. J. Wold and C. D. Frisbie, *J. Am. Chem. Soc.* 123, 5549 (2001).
- D. J. Wold, R. Haag, M. A. Rampi, and C. D. Frisbie, *J. Phys. Chem. B* 106, 2813 (2002).
- X. D. Cui, X. Zarate, J. Tomfohr, O. F. Sankey, A. Primak, A. L. Moore, T. A. Moore, D. Gust, G. Harris, and S. M. Lindsay, *Nanotechnology* 13, 5 (2002).
- X. D. Cui, A. Primak, X. Zarate, J. Tomfohr, O. F. Sankey, A. L. Moore, T. A. Moore, D. Gust, L. A. Nagahara, and S. M. Lindsay, *J. Phys. Chem. B* 106, 8609 (2002).
- R. Holmlin, R. Haag, M. L. Chabinyc, R. F. Ismagilov, A. E. Cohen, A. Terfort, M. A. Rampi, and G. M. Whitesides, *J. Am. Chem. Soc.* 123, 5075 (2001).
- M. A. Rampi and G. M. Whitesides, *Chem. Phys.* 281, 373 (2002).
- K. Slowinski, H. K. Y. Fong, and M. Majda, *J. Am. Chem. Soc.* 121, 7257 (1999).
- R. L. York, P. T. Nguyen, and K. Slowinski, *J. Am. Chem. Soc.* 125, 5948 (2003).
- W. Wang, T. Lee, and M. A. Reed, *Phys. Rev. B* 68, 035416 (2003).
- H. R. Jacobs, *Mathematics: A Human Endeavor*, 3rd edn., W. H. Freeman (1994).

22. W. F. Reus, C. A. Nijhuis, J. R. Barber, M. M. Thuo, S. Tricard, and G. M. Whitesides, *J. Phys. Chem. C* 116, 6714 (2012).
23. G. Casella and R. L. Berger, *Statistical Inference*, Duxbury Press, Belmont, CA (1990).
24. P. R. Bevington and D. K. Robinson, *Data Reduction and Error Analysis for the Physical Sciences*, 3rd edn., McGraw-Hill, New York (2003).
25. J. L. Vardeman and S. B. (eds.), *Methods of Experimental Physics Series 28*, Academic Press, San Diego, CA (1994).
26. P. J. Huber, *Robust Statistics*, Wiley Series in Probability and Mathematical Statistics, Wiley and Sons, New York (1981).
27. G. Upton and I. Cook, *Understanding Statistics*, Oxford University Press (1996), Vol. 55.
28. D. Zwillinger and S. Kokoska, *CRC Standard Probability and Statistics Tables and Formulae*, CRC Press (2000), Vol. 18.
29. K. Seo and H. Lee, *ACS Nano* 3, 2469 (2009).
30. A. M. Nardes, M. Kemerink, R. A. J. Janssen, J. A. M. Bastiaansen, N. M. M. Kiggen, B. M. W. Langeveld, A. J. J. M. van Breemen, and M. M. deKok, *Adv. Mater.* 19, 1196 (2007).

Received: 5 November 2013. Accepted: 29 May 2014.

Delivered by Publishing Technology to: Dental Library Seoul Natl Univ
IP: 147.46.182.248 On: Thu, 01 Jan 2015 01:28:18
Copyright: American Scientific Publishers